Laser-induced splittings in the nuclear magnetic resonance spectra of the rare gases

Rodolfo H. Romero*

Laboratory for Instruction in Swedish, Department of Chemistry, P.O. Box 55, A. I. Virtasen aukio 1, FIN-00014 University of Helsinki, Finland

Juha Vaara[†]

Laboratory of Physical Chemistry, Department of Chemistry, P.O. Box 55, A. I. Virtasen aukio 1, FIN-00014 University of Helsinki, Finland (Dated: October 13, 2018)

Circularly polarized laser field causes a shift in the nuclear magnetic resonance (NMR) spectra of all substances. The shift is proportional to the intensity of the laser beam and yields oppositely signed values for left- and right-circularly polarized light, CPL -/+, respectively. Rapid switching — in the NMR time scale — between CPL+ and CPL- gives rise to a splitting of the NMR resonance lines. We present uncorrelated and correlated quadratic response calculations of the splitting per unit of beam intensity in the NMR spectra of 21 Ne, 83 Kr, and 129 Xe. We study both the regions far away from and near to optical resonance and predict off-resonance shifts of the order 0.01, 0.1, and 1×10^{-6} Hz for 21 Ne, 83 Kr, and 129 Xe, respectively, for a beam intensity of 10 W/cm². Enhancement by several orders of magnitude is predicted as the beam frequency approaches resonance. Only then can the effect on guest 129 Xe atoms be potentially useful as a probe of the properties of the host material.

Nuclear magnetic resonance (NMR) spectroscopy has become one of the most successful techniques for the analysis of molecular structure [1]. Irradiation by circularly polarized light (CPL) from a laser has been proposed as a potentially useful technique of enhancing the resolution of NMR spectra [2]. Early experiments searching for the effect, in a solution of chiral molecules, reported shifts of the order of 1 Hz in a 270 MHz NMR spectrum [3]. Much of that magnitude can, however, be explained by heating effects and only a residual of at most 0.1 Hz could be interpreted as originating in other mechanisms [4]. Theory for the laser field-induced NMR shifts was presented by Buckingham and Parlett [5, 6], in terms of the inverse Faraday effect [7], i.e., induced magnetization caused by the CPL beam propagating through any sample. Since the laser-induced shifts become proportional to the square of the electric field of the laser or, equivalently, the intensity of the beam [5, 6, 8], initial proposals involved using high-intensity pulsed lasers to obtain shifts of the order of GHz [2]. This is, however, ruled out in NMR experiments, even leaving aside the heating problem, due to the long lifetime of the nuclear spin states. Hence, intensities of the order of tens of W/cm², obtainable from continuous wave lasers, must be considered in estimates of the order of magnitude of the induced shifts. Left- and right-circularly polarized light cause opposite shifts. If the laser field is switched between the two modes rapidly in the NMR time scale, the spectral lines are doubled, with splitting proportional

to the beam intensity.

NMR of guest rare gas atoms can be used as a sensitive probe of the microstructure of the surrounding medium [9]. In this work, we present *ab initio* electronic structure calculations of the laser-induced splitting per unit of beam intensity in the NMR spectra of free atomic ²¹Ne, ⁸³Kr, and ¹²⁹Xe, both at frequencies away from and near to optical resonance. In the off-resonance region, at standard laser wave lengths and intensities, the splittings in ¹²⁹Xe are below the limit of current experimental capabilities, while a large enhancement is expected when approaching resonance.

A CPL beam of frequency ω induces a magnetic field at the position of the nucleus K in a molecule given by [5, 6]

$$B_{K,\alpha}^{\pm} = \frac{1}{2\omega} b_{\alpha\beta\gamma}^{K} \left(E_{\beta}^{\pm} \dot{E}_{\gamma}^{\pm} - E_{\gamma}^{\pm} \dot{E}_{\beta}^{\pm} \right). \tag{1}$$

Here, E^{\pm} represents the electric field of the right (+) or left (-) circularly polarized beam, and $b_{\alpha\beta\gamma}^{K}$ can be calculated as a third-order perturbation expression from [10]

$$b_{\alpha\beta\gamma}^{K} = -\frac{\alpha^{2}}{2} \operatorname{Im}\langle\langle\sum_{i} \frac{\ell_{iK,\alpha}}{r_{iK}^{3}}; r_{\beta}, r_{\gamma}\rangle\rangle_{\omega,-\omega}, \qquad (2)$$

where we have used atomic units and the notation for the quadratic response function [11] $\langle \langle A; B, C \rangle \rangle_{\omega_1,\omega_2}$, equivalent to time-dependent third-order perturbation theory with the time-dependent operators B and C, as well as their respective frequencies ω_1 and ω_2 . In Eq. (2), α is the fine structure constant, r_{β} and r_{γ} are the components of the electric dipole moment, r_{iK} is the distance between the electron i and the nucleus K, and $\ell_{iK,\alpha}$ is the α component of the angular momentum of the electron i around the nucleus K. While $-\alpha^2 \sum_i \ell_{iK}/r_{iK}^3$ is the magnetic field at nucleus K due to the orbital motion of the electrons, Eq. (2) corresponds to the modification

^{*}Electronic address: rodolfo@chem.helsinki.fi; Permanent address: Department of Physics, Facultad de Ciencias Exactas y Naturales, Universidad Nacional del Noredeste, Avenida Libertad 5500, (3400) Corrientes, Argentina. email: rhromero@exa.unne.edu.ar

 $^{^{\}dagger}$ Electronic address: jvaara@chem.helsinki.fi

of this quantity by the external, time-dependent electric field.

The relevant quantity for NMR experiments in the isotropic gas or liquid phase is the isotropic rotational average

$$b_K = \frac{1}{6} \sum_{\alpha\beta\gamma} \epsilon_{\alpha\beta\gamma} b_{\alpha\beta\gamma}^K = \frac{1}{3} \left(b_{xyz}^K + b_{yzx}^K + b_{zxy}^K \right), \quad (3)$$

where $\epsilon_{\alpha\beta\gamma}$ stands for the Levi-Civita tensor and (x,y,z) is the molecule-fixed Cartesian frame. For spherically symmetric systems, Eq. (3) reduces to one of the components of $b_{\alpha\beta\gamma}^K$, e.g. b_{xyz}^K . The induced field is stationary and oriented along the direction of propagation of the beam. It couples to the magnetic moment $\gamma_K \mathbf{I}_K$ of nucleus K, to give a term in the NMR spin Hamiltonian (in frequency units) in the high-field approximation as

$$H_{\text{NMR}} = \pm \frac{1}{4\pi} \gamma_K I_{K,Z} b_K E_0^2, \tag{4}$$

where γ_K is the magnetogyric ratio of K, $I_{K,Z}$ is the component of I_K along the external magnetic field, and E_0 is the amplitude of the electric field associated with the laser beam. Eq. (4) corresponds to equally large but oppositely directed frequency shifts, Δ and $-\Delta$, for the two differently polarized beams. Δ depends on the intensity I_0 of the beam, and becomes [12]

$$\Delta = \frac{1}{4\pi c\epsilon_0} \gamma_K b_K I_0, \tag{5}$$

where c and ϵ_0 are the speed of light and permittivity of vacuum, respectively.

Calculations of Δ/I_0 were performed with the DAL-TON program [13], using the implementations of analytic quadratic response functions of Ref. 14 at the ab initio self-consistent field (SCF) and multiconfiguration SCF (MCSCF) levels, and Ref. 15 using density-functional theory (DFT). We studied the basis set convergence of the laser-induced shifts, starting with the uncontracted Gaussian basis set denoted by HIVu in Ref. [16]. Diffuse (small-exponent) functions were added to each block of angular momentum until convergence of the results at the correlated MCSCF level [using the complete active space (CAS) [17] wave function specified in Table I] to within 0.1% was reached. This procedure has been shown to lead to results close to the basis set limit in the calculation of nuclear magnetic shielding constants of the rare gases [18]. The final, converged basis sets are $(15s \, 11p \, 7d \, 5f)$, $(19s \, 16p \, 15d \, 5f)$, and $(26s \, 20p \, 16d \, 3f)$ for Ne, Kr and Xe, respectively. All the results reported below correspond to these converged basis.

Both CAS and restricted active space (RAS) [19] -type MCSCF wave functions were used. The details of the chosen active spaces are given in Table I. The three-parameter hybrid B3LYP functional [20] was used in the DFT calculations. The calculations were performed for a set of typical laser frequencies. We also calculated the lowest singlet excitation energies for each atom with a

CASSCF wave function, to estimate the range of frequencies where optical resonances occur. These ranges are 0.63–1.05 a.u. for Ne, 0.41–0.52 a.u. for Kr, and 0.35–0.45 a.u. for Xe. Δ/I_0 was evaluated at frequencies approaching the resonance, too.

The results for Δ/I_0 in $^{21}{\rm Ne}$, $^{83}{\rm Kr}$ and $^{129}{\rm Xe}$ are presented in Table II. The range of the shifts, calculated at SCF level, due to a laser beam intensity of $10~{\rm W/cm^2}$ and wavelengths between 13190 and 4880 Å, is 1.7– $4.7~{\rm nHz}$ for $^{21}{\rm Ne}$, 9.6– $30~{\rm nHz}$ for $^{83}{\rm Kr}$, and 80– $290~{\rm nHz}$ for $^{129}{\rm Xe}$. The corresponding values for $^{131}{\rm Xe}$ are of the opposite sign and smaller than those for $^{129}{\rm Xe}$, and can be obtained from the latter by multiplying by the quotient of the respective magnetogyric ratios $\gamma_{^{131}{\rm Xe}}/\gamma_{^{129}{\rm Xe}}=-0.296$.

Inclusion of electron correlation at the CAS level increases Δ/I_0 by about about 15% for Ne, but decreases it by ca. 20% for Kr and Xe. Comparison of the results obtained with the different RAS and CAS wave functions shows that the choice of the active space is more important than using the multireference (CAS) wave functions. With RAS wave functions, correlation increases the shifts by up to around 15% for Ne and 25% for Kr and Xe, compared to the SCF level. For all atoms and frequencies, the DFT/B3LYP results are significantly larger than those corresponding to the ab initio methods. We have also tested the LDA and BLYP functionals, which resulted in even larger shifts.

The larger shifts obtained for Xe as compared to Ne and Kr can be attributed to the larger polarizability of xenon. The electron cloud is deformed in response to the external electric field, thus giving a corresponding larger induced magnetic field at the nuclear site. Results of correlated CAS calculations of Δ/I_0 and the dynamic polarizability $\alpha(\omega)$, for Ne, Kr, and Xe as a function of the laser frequency ω , are depicted in Fig. 1. The frequency ranges from 0.1 a.u. to near the threshold of optical resonance, where the properties diverge because of the poles in linear and quadratic response functions. The growth of Δ/I_0 with ω , although qualitatively similar to $\alpha(\omega)$, is faster than in the latter property. There is an enhancement of Δ/I_0 by several orders of magnitude when optical resonance is approached.

Finally, we have also carried out a preliminary investigation of the influence of relativistic effects on Δ , by including the mass-velocity $H^{\mathrm{mv}} = -\frac{1}{8} \, \alpha^2 \sum_i \nabla_i^4$, and Darwin $H^{\mathrm{Dar}} = \frac{1}{2} \, \alpha^2 \pi \sum_K Z_K \sum_i \delta(r_{iK})$ Hamiltonians as additional perturbations. The relativistic corrections

$$b_K^{\text{mv}} = -\frac{\alpha^2}{2} \operatorname{Im} \langle \langle \sum_i \frac{\ell_{iK,x}}{r_{iK}^3}; y, z, H^{\text{mv}} \rangle \rangle_{\omega, -\omega, 0}, \quad (6)$$

$$b_K^{\text{Dar}} = -\frac{\alpha^2}{2} \operatorname{Im} \langle \langle \sum_i \frac{\ell_{iK,x}}{r_{iK}^3}; y, z, H^{\text{Dar}} \rangle \rangle_{\omega,-\omega,0}.$$
 (7)

were evaluated using cubic response functions [21] at the CAS level. The corresponding corrections to the shifts, $\Delta^{\rm mv}$ and $\Delta^{\rm Dar}$, have opposite signs and partially cancel each other. As expected, the relativistic effects

in $^{21}\mathrm{Ne}$ are completely negligible. For $^{83}\mathrm{Kr},~b_K^{\mathrm{mv}}$ and b_K^{Dar} represent, individually, corrections of the same order of magnitude as the uncorrected value of b_K , although their partial cancellation finally leads to values approximately 25% larger than the nonrelativistic value. Finally, $b_{\mathrm{Xe}}^{\mathrm{mv}}$ and $b_{\mathrm{Xe}}^{\mathrm{Dar}}$ are larger than the nonrelativistic values, roughly by a factor of three. Their cancellation leads to a corrected value of about -50 nHz for all the frequencies studied, with $I_0 = 10 \text{ W/cm}^2$. No definitive conclusions may be drawn based on these results, however, as the response functions retain their nonrelativistic pole structure in this approach. Furthermore, picture change effects [22] on the hyperfine operator are also presently neglected. A fully relativistic quadratic response calculation would be more appropriate, and will be pursued in the future.

In summary, we have calculated the shifts induced by circularly polarized laser beam, to the NMR spectra for atomic ²¹Ne, ⁸³Kr, and ¹²⁹Xe using first principles electronic structure methods. At typical beam intensities

and laser frequencies, the shifts are much too small for observation, with the shift for 129 Xe predicted at the order of magnitude of 1 μ Hz. Experimental techniques exploiting higher beam frequencies would benefit from the dramatic enhancement expected at near-resonant frequencies. If realised experimentally, the effect may provide a new characteristic signature of molecular structure in NMR spectroscopy.

M. Jaszuński (Warsaw), A. Rizzo (Pisa), J. Lounila (Oulu), and J. Jokisaari (Oulu) are thanked for useful discussions, as well as T. Helgaker (Oslo) and P. Sałek (Stockholm) for providing a pre-release DFT version of the Dalton software. Financial support from the Magnus Ehrnrooth Foundation (RHR), the Emil Aaltonen Foundation (JV), and the Academy of Finland (RHR and JV, benefiting also from the project 206001 of J. Jokisaari) has been received. RHR is on leave from the Universidad Nacional del Nordeste (Argentina). Computational resources were partially provided by the Center for Scientific Computing, Espoo, Finland.

- A. Abragam, The Principles of Nuclear Magnetism (Oxford University Press, Oxford, 1961); C. P. Slichter, Principles of Magnetic Resonance, 2nd ed. (Springer, Berlin, 1990).
- [2] M. W. Evans, J. Phys. Chem. 95, 2256 (1991).
- [3] W. Warren, Science **255**, 1683 (1992).
- [4] W. Warren, Mol. Phys. 93, 371 (1998).
- [5] A. D. Buckingham and L. C. Parlett, Science 264, 1748 (1994).
- [6] A. D. Buckingham and L. C. Parlett, Mol. Phys. 91, 805 (1997).
- [7] J. P. van der Ziel, P. S. Pershan, and L. D. Malmstrom, Phys. Rev. Lett. 15, 190 (1965).
- [8] R. A. Harris and I. Tinoco, Jr., J. Chem. Phys. 101, 9289 (1994).
- [9] J. Jokisaari, in Encyclopedia of Spectroscopy and Spectrometry, edited by J. C. Lindon, G. E. Tranter, and J. L. Holmes (Academic Press, 2000), and references therein.
- [10] M. Jaszuński and A. Rizzo, Mol. Phys. 96, 855 (1999).
- [11] J. Olsen and P. Jørgensen, Modern Electronic Structure Theory, Part II, edited by D. R. Yarkony (World Scientific, Singapore, 1995); J. Olsen and P. Jørgensen, J. Chem. Phys. 82, 3225 (1985).
- [12] To change from atomic units to SI units we use the equivalence 1 a.u. of $b = mea_0^3/\alpha\hbar^2c = 8.889238\times10^{-19} \text{ s V}^{-1}$.
- [13] T. Helgaker et al., Dalton, a molecular electronic structure program, Release 1.2, University of Oslo, 2001.
- [14] H. Hettema, H. J. Aa. Jensen, P. Jørgensen, and J. Olsen, J. Chem. Phys. 97, 1174 (1992).
- [15] P. Salek, O. Vahtras, T. Helgaker, and H. Ågren, J. Chem. Phys. 117, 9630 (2002).
- [16] J. Vaara, P. Manninen, and J. Lounila, Chem. Phys. Lett. 372, 750 (2003).
- [17] B. O. Roos, P. R. Taylor, and P. E. M. Siegbahn, Chem. Phys. 48, 157 (1980).
- [18] J. Vaara and P. Pyykkö, J. Chem. Phys. 118, 2973 (2003).

- J. Olsen, B. O. Roos, P. Jørgensen, and H. J. Aa. Jensen,
 J. Chem. Phys. 89, 2185 (1988); P.-Å. Malmqvist,
 A. Rendell, and B. O. Roos, J. Phys. Chem. 94, 5477 (1990).
- [20] A. D. Becke, J. Chem. Phys. 98, 5648 (1993);
 P. J. Stephens, F. J. Devlin, C. F. Chabalowski, and M. J. Frisch, J. Phys. Chem. 98, 11623 (1994).
- [21] D. Jonsson, P. Norman, and H. Ågren, J. Chem. Phys. 105, 6401 (1996).
- [22] M. Barysz and A. J. Sadlej, Theor. Chim. Acta 97, 260 (1997); V. Kellö and A. J. Sadlej, Int. J. Quantum Chem. 68, 159 (1998).

TABLE I: Active atomic orbital spaces of the MCSCF wave functions used.

Atom	Wave Function	$N_e{}^a$	Active Space
Ne	CAS	8	$2s2p \rightarrow 3s3p3d$
	RAS-I	8	$2s2p \rightarrow 3s3p3d$
	RAS-III	10	$1s2s2p \rightarrow 3s3p3d4s4p4d4f5s5p$
Kr	CAS	8	$4s4p \rightarrow 4d$
	RAS-I	8	$4s4p \rightarrow 4d$
	RAS-II	18	$3d4s4p \rightarrow 4d4f5s5p5d$
	RAS-III	26	$3s3p3d4s4p \rightarrow 4d4f5s5p5d5f6s6p$
Xe	CAS	8	$5s5p \rightarrow 5d$
	RAS-I	8	$5s5p \rightarrow 5d$
	RAS-II	18	$4d5s5p \rightarrow 4f5d6s6p6d$
	RAS-III	26	$4s4p4d5s5p \rightarrow 4f5d5f6s6p6d7s7p$

 $^{^{}a}$ N_{e} is the number of correlated electrons.

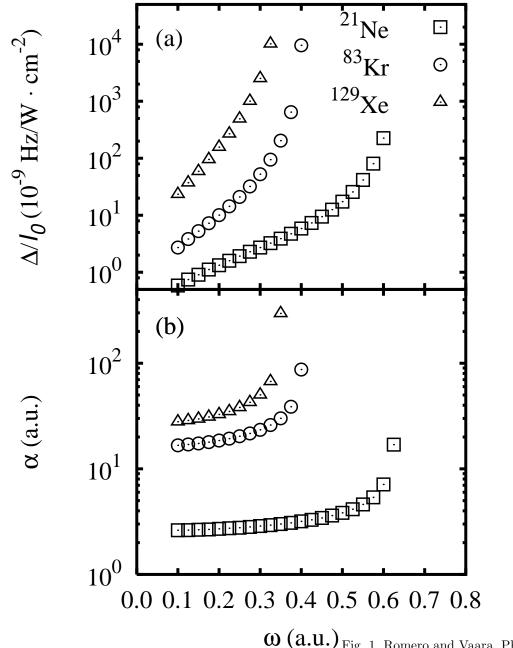
TABLE II: Calculated laser-induced NMR line shifts per unit of laser beam intensity, Δ/I_0 [in $10^{-9}~{\rm Hz/(W\,cm^{-2})}]$ in rare gas atoms Ne, Kr, and Xe.

Nucleus	ω^a (a.u.)	SCF	CAS	RAS-I	RAS-II	RAS-III	B3LYP
²¹ Ne	0.0345439	0.17	0.19	0.19	_	0.19	0.31
	0.0428227	0.21	0.24	0.23	_	0.24	0.38
	0.0656249	0.32	0.37	0.36	-	0.37	0.60
	0.0773571	0.38	0.44	0.43	_	0.44	0.71
	0.0885585	0.44	0.51	0.50	_	0.51	0.83
	0.0932147	0.47	0.53	0.52		0.53	0.87
$^{83}{ m Kr}$	0.0345439	0.96	0.80	0.80	0.85	1.49	1.76
	0.0428227	1.17	1.01	1.01	1.06	1.86	2.24
	0.0656249	1.92	1.60	1.60	1.76	2.98	3.62
	0.0773571	2.34	1.97	1.97	2.13	3.57	4.42
	0.0885585	2.82	2.34	2.34	2.56	4.26	5.27
	0.0932147	2.98	2.50	2.50	2.77	4.53	5.70
$^{129}\mathrm{Xe}$	0.0345439	7.99	5.32	5.32	9.58	10.65	19.17
	0.0428227	10.11	6.92	6.92	12.25	13.31	24.50
	0.0656249	17.04	12.25	12.25	20.24	22.90	41.00
	0.0773571	21.83	15.44	15.44	25.56	28.22	51.12
	0.0885585	26.62	19.17	19.70	31.42	34.61	62.84
	0.0932147	29.29	20.77	21.30	34.08	37.81	68.16

 $[^]a$ The frequencies correspond to wavelengths $\lambda=13190,$ 10640, 6943, 5890, 5145, and 4888 Å, in the respective order.

FIGURE CAPTIONS

FIG. 1: Results of correlated CAS calculations of (a) the laser-induced NMR shift per unit of beam intensity Δ/I_0 , and (b) frequency-dependent polarizability $\alpha(\omega)$, as a function of the frequency ω , for atomic Ne, Kr, and Xe.



 ω (a.u.) $_{\rm Fig.~1,~Romero~and~Vaara,~Phys.~Rev.~A.}$